THE SOLAR LITHIUM ABUNDANCE

I: *Observations of the Solar Lithium Feature at λ6707.8 Å*

JAMES W. BRAULT

Kitt Peak National Observatory,* Tucson, Ariz., U.S.A.

and

EDITH A. MÜLLER**

Observatoire de Genève, Switzerland

Abstract. A detailed observational study of the solar photospheric lithium feature has been carried out with emphasis on center-limb observations, continuum location, possible effects of telluric lines, effects of blending by atomic and molecular lines, and decomposition of the solar spectrum around λ6707 Å.

1. Introduction

The precise determination of the lithium abundance in the solar atmosphere has been an intriguing problem in recent years because of its implications on problems of nucleosynthesis and stellar evolution. Different observers have derived widely different results for the quivalent width of the lithium resonance doublet at λ6707.8, ranging from 7.41 mÅ (Mutschlecner, 1963) down to <0.61 mÅ (Peach, 1968). Daehler (1967) even doubted the presence of lithium in the photospheric spectrum. A review of the results is given by Grevesse (1968).

The reason for the discrepant results is basically twofold. (1) The observations are difficult because the resonance lines are extremely weak, the greatest central depth of the lithium feature being $\sim 1\%$. No other lithium line is observable in the visible photospheric spectrum. (2) The analysis is hampered by the possible presence of atomic, molecular and telluric lines within the lithium feature.

We felt that new observations of high precision could remove most of the uncertainties of previous studies. These new observations included (1) a wide range in wavelength for placing the continuum, (2) scans at high and low Sun to check on possible telluric blendings, (3) scans at different center-limb positions to disentangle blends, and (4) laboratory measurements as an aid to identifications.

2. Technique of Observation and Reduction

The photoelectric observations of the Li ɪ resonance doublet at λ6707.8 Å were secured with the McMath solar telescope and spectrometer of the Kitt Peak National Obser-

vatory. The plane grating spectrometer of the Czerny-Turner type was used in the double pass arrangement with a prismatic predisperser placed in front of the entrance slit to eliminate overlapping orders.

One observational record of a particular spectral region consists of an integration over a great number of spectral scans which are accomplished by rotating the grating over the desired length of the spectrum. The scattered light in the main spectrograph is corrected for by scanning alternatively (1) the solar spectrum in the forward motion of the grating rotation and (2) the scattered light in the backward motion of the grating after closing the intermediate slit. The scattered light scan is then simply subtracted from the solar spectrum. The photomultiplier signal is digitized and transmitted to an electronic computer which collects and processes the data. The output data are recorded on magnetic tape for further processing. A detailed description of the spectrometer in its double pass mode is given by Brault *et al.* (1971). The observed line profiles are converted to true solar line profiles by means of the Fast Fourier Transform technique (Brault and White, 1971).

3. Observations of the Solar Lithium Feature

A detailed study of the photospheric lithium lines requires a set of observations of the region around $\lambda 6707.8$ Å made at various positions across the solar disk and secured under excellent atmospheric conditions. Several attempts were made to obtain such a set of data. The present analysis is based on observations secured at a time when the peak to peak motion of the 80 cm solar image due to atmospheric turbulence was between 1 and 2″, the least motion occurring during the observations near the limb of the Sun. The entrance slit was 20 mm long and 100 μ wide which projected on to the solar image corresponds to 50 by 0.25″.
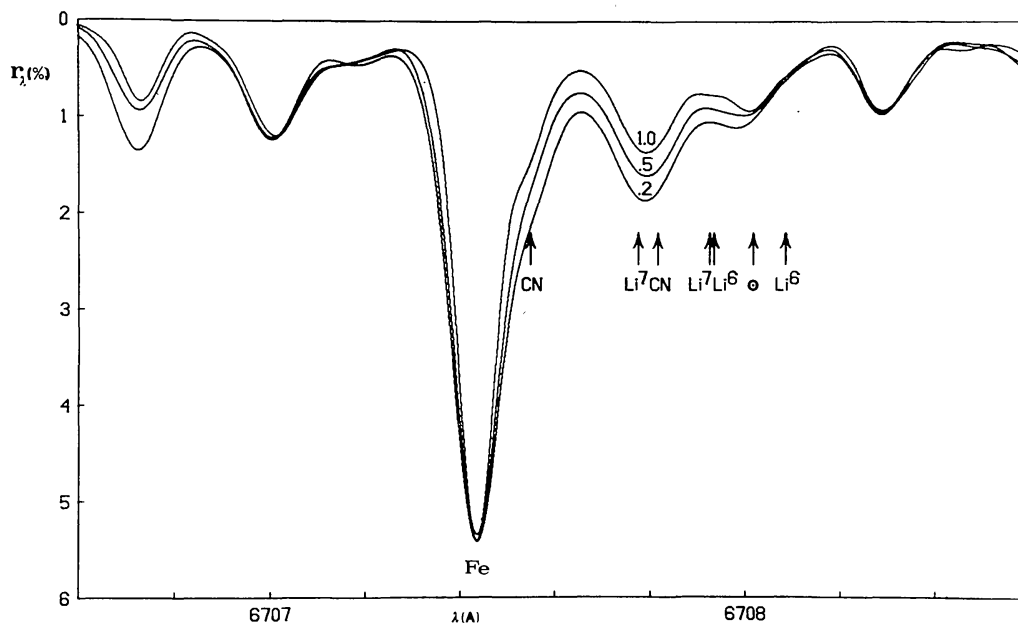

Fig. 1.   The solar lithium feature as observed at three positions on the solar disk ($\mu = 1.0, 0.5$, and 0.2).

The observations were made at the following positions on the solar disk: $\mu = 1.0$, 0.8, 0.5, 0.4, 0.3 and 0.2. When selecting the positions on the disk great care was taken to avoid active regions. At the chosen positions no plages were detectable on the H-α spectroheliogram secured at the same time. Thus, our observations refer to the undisturbed photosphere.

Each spectral record of the lithium feature at every μ-position represents an integration of 200 scans of a region of the solar spectrum 6 Å in length centered at $\lambda 6707.6$ Å. To secure 200 scans over 6 Å in length required 27 min of time at any particular μ-position. The great number of scans is necessary to produce low noise spectra of very faint solar lines. Figure 1 illustrates the Li I feature recorded at $\mu = 1.0$, 0.5 and 0.2. The three profiles are superimposed in such a way that the centers of the $\lambda 6707.43$ Å line coincide. The profiles observed at the other μ-positions fit very regularly in between the profiles shown here.

Several additional observations are required for the detailed analysis of the solar Li I lines. We describe them in the following paragraphs.

4. Location of the Continuum

Since the lithium lines appear as very faint absorption features in the solar spectrum, it is essential to determine the position of the continuum as reliably as possible. For this purpose we recorded the solar spectrum over a range of about 75 Å centered at around 6707 Å both at the center and near the limb ($\mu = 0.2$) of the solar disk. Nu-
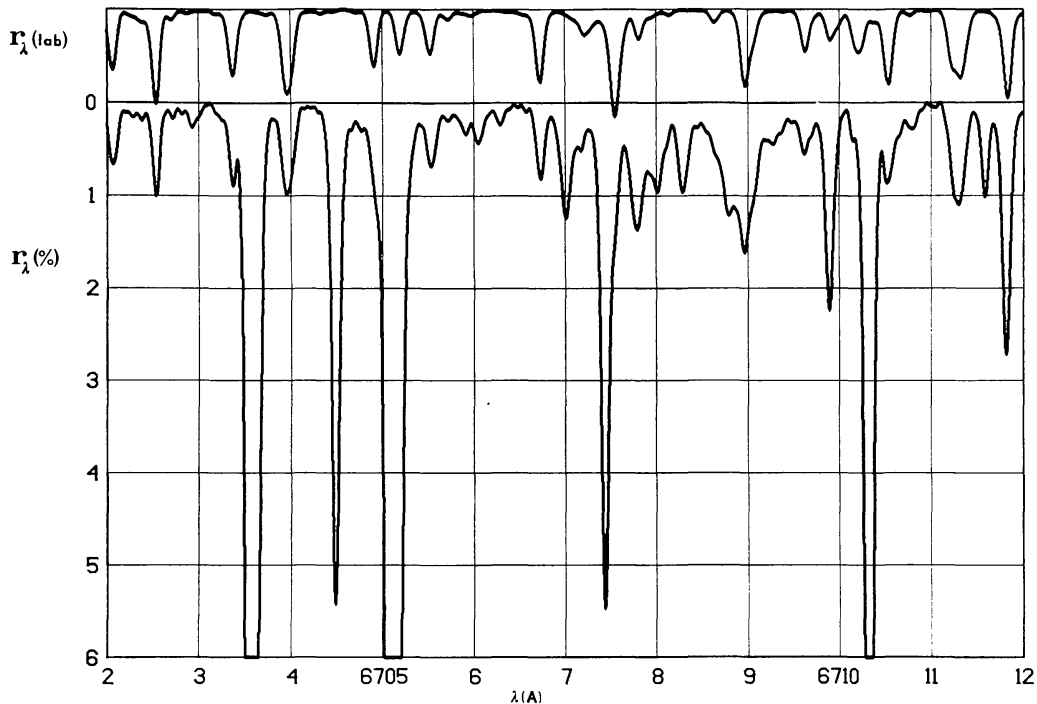

Fig. 2. Upper tracing: the CN arc spectrum between $\lambda 6702$ and 6712 Å. Lower tracing: the solar spectrum of the same wavelength region at $\mu = 1.0$. Only the first 6% of the solar intensity scale down from the continuum are reproduced.

merous faint lines appear on our high dispersion low noise spectra which, obviously, must be taken into consideration when tracing the continuum. Many of these faint lines are due to solar CN and change appreciably in intensity across the solar disk. In order to fix the position of the continuum we have selected the highest points between absorption lines which remain unchanged from center-to-limb.

The location of the continuum thus determined is shown in the lower portion of Figure 2 which represents the region $\lambda6702$ to 6713 Å recorded at the disk center. Only the first 6% of the intensity scale below the continuum are shown on Figure 2.

The position of the continuum as we have determined it on our solar spectral tracings lies appreciably higher than the continuum location proposed by several authors in recent years. For example, Daehler (1967) and Peach (1968) place the continuum very near to the peak at $\lambda6707.65$ Å near the lithium feature. However, our continuum location appears to be in good agreement with the observations by Delbouille and Roland which Grevesse (1968) employed in his study.

5. Atmospheric Lines

To ascertain that no atmospheric lines contribute to the solar lithium absorption we recorded the solar spectrum over a wavelength range of more than 30 Å centered at $\lambda6707$ Å both at high and low Sun positions. Several faint atmospheric lines showed up on the low Sun spectra. The strongest of them that fall in the neighborhood of the lithium feature has a wavelength of $\lambda6706.07$ Å and a central intensity of 0.06% per precipitable centimeter of water. No atmospheric lines were found to coincide with the lithium feature itself. The lithium feature of the low Sun spectrum is identical with that of the high Sun spectrum. Thus a possible blending of atmospheric lines within the lithium feature is ruled out.

6. The Position of the Li I Lines in the Solar Spectrum

The precise position of the Li I resonance doublet in the solar spectrum of both the Li^7 and the Li^6 isotopes was determined by means of a laboratory comparison spectrum. A lithium hollow-cathode lamp served as laboratory light source. Both the solar and the laboratory Li I spectra were recorded under exactly the same conditions and set-up of the solar spectrograph. The necessary wavelength shifts due to motions of the Earth and the gravitational redshift were then applied to the observed laboratory wavelengths. Thus, the solar wavelengths of the Li I lines of both isotopes were found. The positions of the four Li I lines corresponding to the observations at $\mu=1.0$ are indicated by arrows in Figure 1.

7. Blends with Molecular Lines

Our center-to-limb observations of the solar spectrum in the region between $\lambda6670$ and 6744 Å confirm the existence of numerous molecular lines pertaining to the CN

red system of the $A^2\Pi_r$–$X^2\Sigma^+$ transition which W. S. Benedict had detected on Jung-fraujoch tracings recorded by L. Delbouille and G. Roland (Swensson *et al.*, 1970). The problem then was to know how many CN lines could be found in the region between $\lambda 6707.5$ and 6708.5 Å, and how much of the absorption within the solar lithium feature might actually be due to solar CN.

The most direct way to get an answer to these questions was to record the laboratory spectrum of the red CN system with the Kitt Peak solar spectrograph. A carbon arc in air served as light source. The rotational temperature of the arc proved to be sufficiently similar to that of the Sun that a direct intercomparison is possible. The comparison revealed that many of the solar CN lines are blended with atomic lines. However, a sufficient number of lines can be found in the solar spectrum which are entirely due to CN and which, therefore, can be used to adjust the laboratory intensity scale to the solar spectrum intensity scale. For this purpose we selected a group of five CN lines of the red system around $\lambda 6728$ Å indicated by arrows in Figure 3. In Figure 3 the upper tracing represents the CN arc spectrum and the lower tracing the solar spectrum of which only the first 3% of the intensity scale down from the continuum are reproduced. The spectroscopic data (laboratory wavelength, band, branch and J-value) of the five relevant CN lines are given in Table I. The last column gives the observed equivalent width of each line.
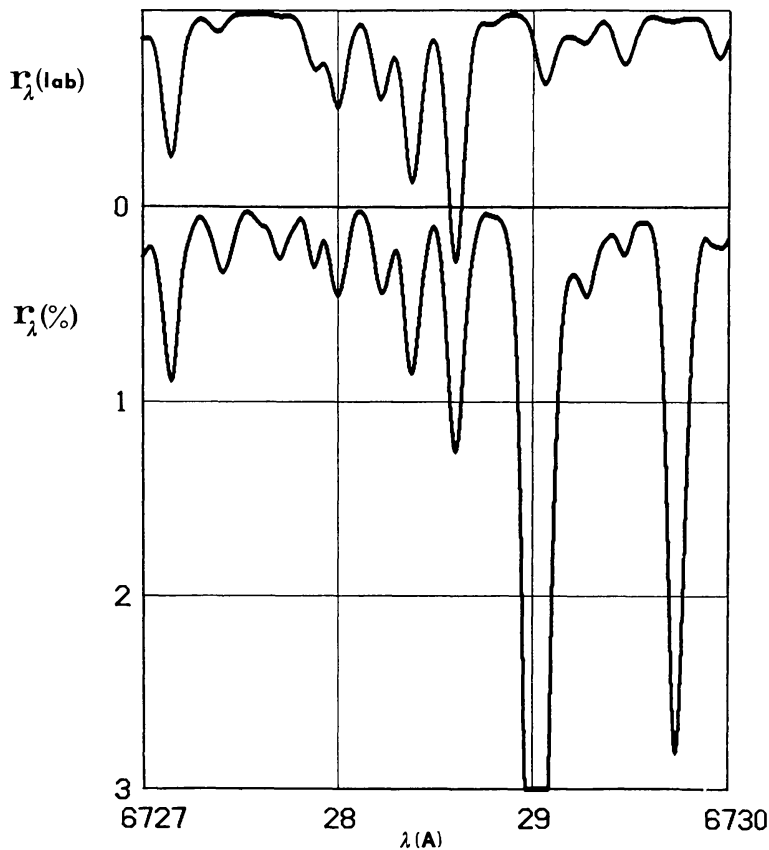

Fig. 3. Upper tracing: the CN arc spectrum between $\lambda 6727$ and $\lambda 6730$ Å. Lower tracing: the solar spectrum of the same wavelength region at $\mu = 1.0$. Only the first 3% of the solar intensity scale down from the continuum are reproduced.

TABLE I

The five CN lines used to fit the CN arc spectrum to the solar spectrum

Line No.	$\lambda_{lab.}$ (Å)	Band v_1-v_2	Branch	J	W_λ (mÅ)
1	6727.873	5–1	P_1	53	0.3
2	27.994	7–3	R_1	33	0.6
3	28.214	7–3	R_2	34	0.5
4	28.375	6–2	Q_2	46	1.0
5	28.597	7–3 / 5–1	Q_1 / Q_1	26 / 59	1.5

Having fitted the arc intensity scale to that of the solar spectrum and applied the necessary shifts to the laboratory wavelengths, the spectra may be directly inter-compared. The upper tracing of Figure 2 reproduces a portion of the CN arc spectrum between $\lambda 6702$ and 6713 Å. It includes the critical wavelengths of the solar lithium feature. When comparing in Figure 2 the arc spectrum with the solar spectrum (lower tracing) we see that, although many faint CN lines appear in the solar spectrum, the CN molecule contributes only little to the absorption within the solar lithium feature.

Near the lithium feature the strongest CN line observed in the arc spectrum has a wavelength of $\lambda 6707.55$ Å. It is composed of five CN lines between $\lambda 6707.50$ and $\lambda 6707.63$ Å (Grevesse, 1968). As shown in Figure 1 this composite CN line falls on the red wing of the $\lambda 6707.44$ Fe I line. Using the CN arc spectrum (upper tracing of Figure 2) we find $W_\lambda = 1.6$ mÅ for the total equivalent width of all five CN components together, the strongest contribution of $W_\lambda = 1.0$ mÅ coming from the 6–2 Q_2 (44)
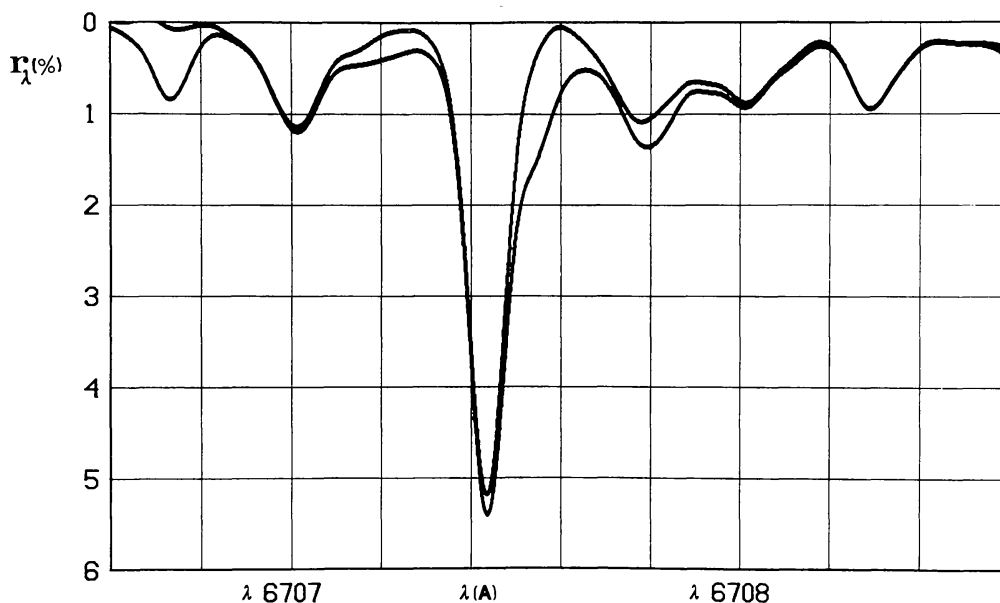

Fig. 4. The solar spectrum around the lithium feature at $\mu = 1.0$, and superimposed on it the solar spectrum after removal of the CN lines.

line. Grevesse (1968) lists three CN lines perturbing directly the lithium lines between $\lambda 6707.75$ Å and $\lambda 6707.83$ Å. The strongest of them is the line 5–1 R_1 (64) for which we find an equivalent width of $W_\lambda = 0.3$ mÅ. The other two lines are extremely faint (Figure 2 upper tracing) and have equivalent widths of 0.05 mÅ or less.

Due to the fact that the solar CN lines near and within the lithium feature are very faint, we may simply subtract the scaled CN laboratory spectrum from that of the Sun. The result is shown in Figure 4 for the region $\lambda 6706.5$–6708.5 Å. We reproduce here the observed solar spectrum and the spectrum as it would appear if no CN lines were present. It clearly can be seen how the CN lines change the shape of the $\lambda 6707.434$ Fe I line and influence the actual lithium feature. Notice that the solar line at $\lambda 6706.72$ Å disappears on the superimposed tracing since it is due to the 7–3 Q_1 (22) transition of the CN red band system.

8. Decomposition of the Solar Lithium Feature

In order to get a feeling for the various components which might contribute to the actual lithium feature, we numerically decomposed the solar spectrum between $\lambda 6706.8$ and $\lambda 6708.6$ Å. To simplify the decomposition we used the solar spectrum deprived of the CN lines, as discussed in Section 7. Since the lines are faint we may represent the spectrum by a superposition of Voigt profiles.

The observed spectrum clearly indicates that the lithium feature contains at least four components. Thus, the simplest assumption is to use four components, assigning two of them to lithium. For each component we must find (a) the central wavelength, (b) the line strength, (c) the Doppler width, and (d) the damping parameter. To reduce the number of free parameters the damping was arbitrarily fixed and the widths of the two presumed lithium components were held at the values predicted by the Holweger
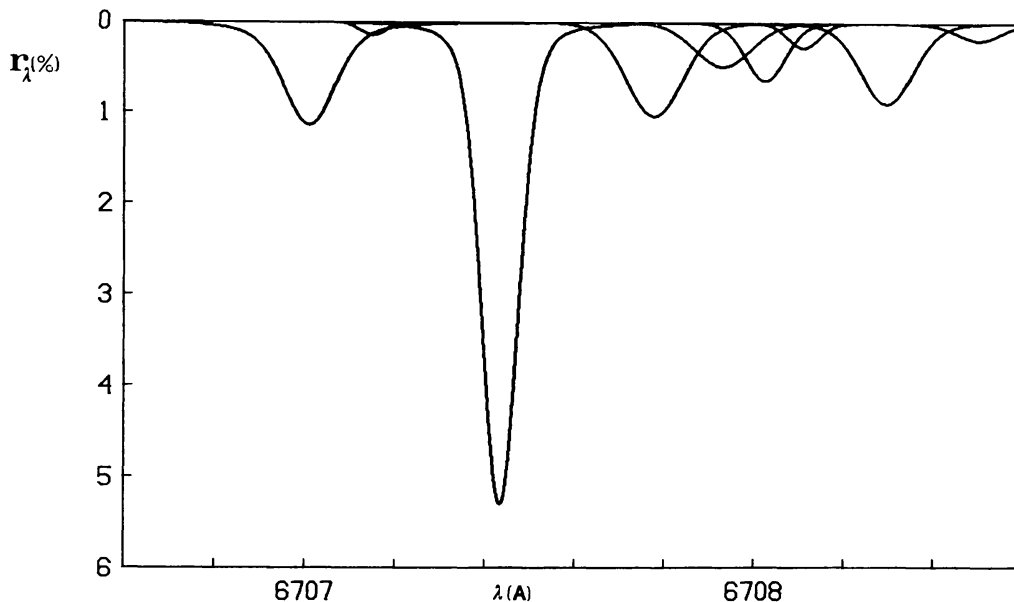

Fig. 5. The decomposed solar spectrum around the lithium feature at $\mu = 1.0$ without CN lines.

TABLE II

The decomposed lithium feature

$\lambda_0(\mu=1.0)$	$\mu=1.0$		$\mu=0.3$		$\mu=0.2$		Identification	Predicted solar λ_0
	$I_{\lambda_0}(\%)$	W_λ(mÅ)	$I_{\lambda_0}(\%)$	W_λ(mÅ)	$I_{\lambda_0}(\%)$	W_λ(mÅ)		
6707.436	5.3	6.0	5.2	6.9	5.2	6.8	Fe I	6707.441
7.778	1.0	1.8	1.5	2.5	1.5	2.5	Li^7	6707.776
7.930	0.5	0.8	0.8	1.4	0.8	1.3	$\{$ Li^7 $\{$ Li^6	6707.927 6707.936
8.025	0.7	0.8	0.8	1.2	0.9	1.4	○	–
8.110	0.3	0.3	0.3	0.4	0.4	0.5	$\{$ Li^6 $\{$ ○	6708.087 –

(1967) model and a macroturbulence of 1.8 km s^{-1}. The intensities and wavelengths were allowed to vary. For the two remaining components only the damping was fixed.

In the final decomposition we may judge the validity of our assumptions by checking the following three requirements:

(1) the synthetic spectrum must fit the observed spectrum at all μ positions;

(2) at $\mu=1.0$ the wavelengths of the individual components must agree with the predicted solar wavelengths (i.e., laboratory wavelengths corrected for the Earth's motion and the gravitational red shift) of the identified lines;

(3) the intensity ratio of the two presumed lithium components must remain constant from center-to-limb.

Figure 5 illustrates the final decomposition of the solar spectrum deprived of CN lines at $\mu=1.0$. Similar decompositions were obtained for the observations at various positions on the solar disk. We found that the rms deviation of the synthetic spectrum and the observed spectrum is of the order of 0.03%. Thus our first requirement is satisfied.

In Table II we list the central intensities (I_{λ_0}) and the equivalent widths (W_λ) of the individual components resulting from the decomposition at $\mu=1.0$, 0.3 and 0.2. The first column gives the wavelength at $\mu=1.0$ of each component. The last column lists the predicted solar wavelengths of the components assuming the identifications given in the preceeding column.

The first line, $\lambda6707.44$, is visible in the Utrecht Atlas and also on many stellar spectra. Its origin remained unknown for a long time but it has recently been identified by Tech (1971) as due to Fe I.

The wavelengths of the next two lines of Table II (the assumed lithium lines) are in excellent agreement with the predicted solar wavelengths. This satisfies our second requirement. The improvement in wavelength agreement of our decomposition compared to that of Daehler (1967) is mainly due to the fact that we have removed the CN lines from the observed solar spectrum before decomposing it.

It should be noted that we have not attempted to further decompose the line at $\lambda6707.930$ Å which may be a composite of the $\lambda6707.927$ line of Li^7 and the $\lambda6707.936$ Å line of Li^6, the two wavelengths being separated by only 0.009 Å. Similarly we did not decompose the line at $\lambda6708.110$ Å which contains an unknown solar line in addition to a possible contribution of the Li^6 line at $\lambda6708.087$ Å. Clearly the line at $\lambda6708.110$ Å cannot be due to Li^6 only. First, it does not have the correct wavelength and, second, the line is too strong compared to the composite line of Li^7+Li^6 at $\lambda6707.930$ Å and to the Li^7 line at $\lambda6707.778$ Å. Furthermore, it cannot be due to iron since Tech (1971) informs us that it is not visible on the laboratory Fe I plate on which the line $\lambda6707.44$ Å appears relatively strong.

In order to check our third requirement we determined the intensity ratio of the two presumed lithium lines (line (1) $\lambda6707.778$ Å, line (2) $\lambda6707.930$ Å) at different μ – values. The ratios of $W_\lambda^{(1)}/W_\lambda^{(2)}$ are 2.1 at $\mu=1.0$, 1.8 at $\mu=0.3$, and 1.9 at $\mu=0.2$, with an uncertainty of about ±0.2 in each value. We conclude that this ratio is ade-

quately constant, so our third requirement is fulfilled. We might mention that the intensity ratio of these two lines indicates that the contribution of Li^6, if any, must be very small since the theoretical ratio of the two Li^7 lines is $2:1$.

9. Conclusions

Our center-to-limb observations definitely support the presence of lithium in the solar spectrum at $\lambda 6707.776$ Å. They also indicate that the presence of CN, while appreciably affecting the apparent lithium wavelengths, contributes only little to the equivalent width of the lithium feature. For the determination of the true continuum wide scans are of critical importance. The low Sun observations proved that telluric lines do not affect the solar lithium feature.

These observations will be used in the subsequent paper to derive the abundance and the isotopic ratio of lithium in the solar atmosphere.

References

Brault, J. W. and White, O. R.: 1971, *Astron. Astrophys.* **13**, 169.
Brault, J. W., Slaughter, C. D., Pierce, A. K., and Aikens, R. S.: 1971, *Solar Phys.* **18**, 366.
Daehler, M.: 1967, *Astrophys. J.* **150**, 667.
Grevesse, N.: 1968, *Solar Phys.* **5**, 159.
Holweger, H.: 1967, *Z. Astrophys.* **65**, 365.
Mutschlecner, J. P.: 1963, Thesis, University of Michigan.
Peach, J. V.: 1968, *Monthly Notices Roy. Astron. Soc.* **139**, 403.
Swensson, J. W., Benedict, W. S., Delbouille, L., and Roland, G.: 1970, *Mem. Soc. Roy. Sci. Liège* **5**.
Tech, J. L.: 1971, *Nat. Bur. Stand. Monograph* **119**, 170.